Solar Energy
and Sustainable Development
Refereed, biannual scientific journal issued by
The Libyan Center for Solar Energy Research and Studies

Design and Performance Analysis of a Ground Level Solar Thermal Accelerated Turbine (GSTAT) for Compact Power Generation

Benlahcene Djaouida[1], and Sellami Ali[1,2*]

[1]Faculty of Science and Technology, University of Tamanghasset, Tamanghasset, Algeria
[2]Materials and Energy Research Laboratory, University of Tamanghasset, Tamanghasset, Algeria

E-***mail:*** **sellamiali2023@gmail.com*

ARTICLE INFO.

Article history:
Received 14 November 2025
Received in revised form 09 Joun 2026
Accepted 09 Joun 2026
Available online 17 August 2026

KEYWORDS

Solar thermal energy; GSTAT system; buoyancy-driven flow; thermal storage; turbine power; CFD analysis; renewable energy.

ABSTRACT

This study analyzes the Ground-Level Solar Thermal Accelerated Turbine (GSTAT) system, a novel solar thermal technology that eliminates tall chimney structures while maintaining efficient energy conversion. The system features a 244 m diameter main collector, 117 m secondary collector, 10 m horizontal turbine, and 5 m crushed gravel thermal storage layer. Mathematical modeling employs Navier-Stokes equations, energy equations with Boussinesq approximation, and k-ε turbulence modeling. Under 1000 W/m² solar insolation, the system achieves 420 K ground surface temperature (112 K rise), accelerating airflow from 1 m/s inlet velocity to 14 m/s at the turbine. The crushed gravel storage layer provides 89.73% collector efficiency and enables extended operation beyond peak solar hours. CFD analysis confirms smooth velocity transitions and optimal thermal gradients throughout the system. Net electrical output reaches 163.35 kW, accounting for turbine efficiency (85%), generator efficiency (92%), and overall system losses (95% efficiency). Economic analysis yields an LCOE of $0.22-0.33/kWh, competitive with conventional solar chimney systems ($0.15-0.30/kWh) while offering reduced construction complexity and land use requirements. The GSTAT system shows particular promise for distributed power generation where tall structures are impractical, providing a scalable alternative to conventional solar updraft towers.

*Corresponding author.

DOI: https://doi.org/10.51646/jsesd.v15i1.1018

تصميم وتحليل أداء توربين معجّل بالطاقة الشمسية الحرارية على مستوى الأرض (GSTAT) لتوليد الطاقة المدمج

بن لحسن جويدة، سلامي علي

ملخص: تتناول هذه الدراسة تحليل نظام التوربين المعجّل بالطاقة الشمسية الحرارية على مستوى الأرض (GSTAT)، وهو تقنية جديدة في مجال الطاقة الشمسية الحرارية تُلغي الحاجة إلى الهياكل العالية للمداخن مع الحفاظ على كفاءة عالية في تحويل الطاقة. يشتمل النظام على مجمّع رئيسي بقطر 244 م، ومجمّع ثانوي بقطر 117 م، وتوربين أفقي بطول 10 م، وطبقة تخزين حراري من الحصى المكسر بسماكة 5 م. يعتمد النموذج الرياضي على معادلات نافييه-ستوكس، ومعادلات الطاقة باستخدام تقريب بوسينسق، إضافة إلى نموذج الاضطراب ε-k. تحت إشعاع شمسي قدره 1000 واط/م^2، يصل النظام إلى درجة حرارة سطح أرضي تبلغ 420 كلفن (ارتفاع 112 كلفن)، مما يؤدي إلى تسريع تدفق الهواء من سرعة ابتدائية 1 م/ث إلى 14 م/ث عند التوربين. توفر طبقة التخزين من الحصى المكسر كفاءة تجميع تصل إلى 89.73% وتُمكّن من استمرار التشغيل بعد ساعات الذروة الشمسية. تؤكد تحليلات CFD وجود انتقالات سلسة للسرعة وتدرجات حرارية مثالية في جميع أنحاء النظام. يبلغ صافي القدرة الكهربائية المنتَجة 163.35 كيلوواط، مع أخذ كفاءة التوربين (85%) والمولد (92%) والخسائر الإجمالية للنظام (95%) في الاعتبار. أسفر التحليل الاقتصادي عن تكلفة مستوى الطاقة (LCOE) تتراوح بين 0.22-0.33 دولار/ك.و.س، وهي منافسة لتكاليف الأبراج الشمسية التقليدية (0.15-0.30 دولار/ك.و.س) مع توفير انخفاض في تعقيد البناء ومتطلبات استخدام الأرض. يُظهر نظام GSTAT إمكانات واعدة خاصة لتوليد الطاقة الموزعة في الحالات التي تكون فيها الهياكل العالية غير عملية، مما يوفّر بديلاً قابلاً للتوسع عن الأبراج الشمسية ذات الدفع الحراري التقليدية.

الكلمات المفتاحية: الطاقة الشمسية الحرارية، نظام GSTAT، التدفق الناتج عن الطفو، التخزين الحراري، طاقة التوربين، تحليل الديناميكا الحرارية الحاسوبية (CFD)، الطاقة المتجددة.

1. INTRODUCTION

The escalating worldwide energy requirements, combined with growing environmental awareness, have stimulated the advancement of cutting-edge renewable energy solutions capable of delivering sustainable and economically feasible power generation alternatives. Solar thermal power systems have established themselves as a viable substitute for traditional fossil fuel-based electricity generation, providing opportunities to utilize plentiful solar resources while reducing environmental degradation. Within the spectrum of solar thermal technologies, solar chimney power plants have garnered significant scientific interest due to their capacity to transform solar thermal energy into electrical power through natural buoyancy-driven air circulation.

The inaugural operational prototype of a solar chimney facility was constructed in Manzanares, Spain, during the early 1980s. This installation featured a chimney structure measuring 195 meters in height with a 5.08-meter radius, complemented by a collector spanning 122 meters in radius and standing 1.85 meters tall [1-4]. The system achieved temperature increases of up to 17°C within the collector area and maintained average updraft velocities of 12 m/s, producing a designed capacity of 50 kW with an actual peak output of 41 kW [5].

Contemporary developments have positioned these systems as renewable alternatives to conventional fossil fuels. The current global energy environment has been significantly influenced by intensifying geopolitical conflicts, which have destabilized energy markets and exposed the fragility of fossil fuel dependency. Energy disruptions resulting from these geopolitical tensions have underscored the critical necessity for clean, robust, and domestically sourced energy technologies that can guarantee energy independence while tackling environmental issues. Given that approximately 1.1 billion individuals globally continue to lack access to dependable electricity supply [6], solar chimney power plants possess considerable potential to support sustainable energy development by leveraging solar power in an economically viable and expandable approach [7].

Solar chimney power plant architecture comprises three primary elements: a transparent collector structure, a ground surface designed for solar energy absorption, and a central chimney tower. Solar irradiation warms the air beneath the collector, establishing a temperature differential that generates buoyancy-driven airflow through the chimney. Turbine generators positioned at the chimney foundation transform the kinetic energy from the airflow into electrical power [8,9]. Initial SCPP research was initiated by Haaf et al. [10,11], who constructed a prototype facility in Manzanares, Spain. The knowledge acquired from this prototype has established a fundamental framework for confirming later experimental and computational investigations [12].

SCPP research has investigated numerous design and operational variables influencing system performance. Studies have extensively examined the effects of turbine specifications, collector and chimney dimensions, and thermal flux on electricity generation [13-17]. Additional research has analyzed external meteorological factors including ambient crosswinds and solar radiation fluctuations [18]. Moreover, thermal energy storage (TES) systems have become essential components in SCPPs, facilitating the storage of solar energy captured by the ground during daylight hours and its discharge during nighttime or overcast conditions. Effective TES implementations can substantially improve the system's capability to produce electricity consistently throughout daily cycles and seasonal variations, thereby enhancing dependability and efficiency [19].

Comparative analyses by Al-Azawiey and Hassan [20] evaluated different materials, including ceramics and black stones, as potential thermal storage candidates to demonstrate their capacity for improving power output. Similarly, Hurtado et al. [21] illustrated the influence of soil density and thermal inertia on energy production, revealing a 10% enhancement in power generation with increased compaction levels. Computational investigations, such as those conducted by Yaswanthkumar and Chandramohan, [22] have examined TES material applications through three-dimensional CFD modeling, though their analyses frequently lack comprehensive optimization methodologies. Experimental research, including work by Ikhlef et al. [19] have further highlighted the importance of thermal storage in improving collector performance and overall system effectiveness.

Contemporary research has continued advancing SCPP performance understanding and thermal storage integration. Mamgain et al. [23] conducted CFD analysis of thermal energy storage in solar chimney installations by modeling the storage layer as porous media. Their findings indicated that materials with superior thermal conductivity, such as sand, are more suitable for thermal storage applications due to their enhanced heat absorption capabilities during daylight periods. Ikhlef et al.[19] experimentally investigated various TES system effects on small-scale SCPP performance in Isparta, Turkey, utilizing a 4.2-meter chimney height and 5.93-meter collector diameter. Their research demonstrated that collector efficiency strongly correlates with thermal storage implementation, with crushed gravel proving to be the optimal

TES material, achieving 89.73% collector efficiency compared to asphalt, sand, and water-filled tube conFigureurations. Similarly, Cuce et al. [24] determined that natural sand and gravel exhibit comparable performance as TES materials in SCPP applications. Their steady-state numerical modeling demonstrated that both materials produce equivalent output power of 41.636 kW for the Manzanares conFigureuration under 800 W/m² radiation conditions. These investigations underscore the critical role of TES material selection and optimization in improving SCPP effectiveness. Nevertheless, they also reveal the necessity for more thorough evaluations of material characteristics and their dynamic behaviors under diverse operating scenarios. Conventional solar updraft installations, while effective in capturing solar thermal energy through natural convection mechanisms, demand considerable infrastructure investment and substantial vertical clearance, restricting their practical deployment across various geographical and economic settings.

This investigation presents the Ground-Level Solar Thermal Accelerated Turbine (GSTAT) system, which introduces a revolutionary approach to solar thermal power generation by tackling the core challenges inherent in conventional solar updraft technologies. Through eliminating tall chimney structure requirements while preserving efficient thermal-to-mechanical energy transformation, GSTAT technology provides a compact, economically feasible solution for distributed power generation. The system's novel dual-collector design generates horizontal airflow acceleration via precisely engineered thermal gradients, facilitating ground-level turbine operation without sacrificing energy extraction performance.

This investigation addresses significant deficiencies in renewable energy infrastructure through developing a scalable solar thermal system that integrates thermal energy storage advantages with modular design concepts. The GSTAT system's effectiveness in arid environments, where solar radiation is plentiful but conventional infrastructure development faces challenges, establishes it as a valuable renewable energy portfolio component. Additionally, the system's capacity for prolonged operation through integrated thermal storage features improves its practical suitability for reliable power generation.

2. MATHEMATICAL MODELING

This section presents a mathematical model for the GSTAT system, incorporating solar radiation, heat transfer, thermal storage, airflow dynamics, turbulence, turbine power extraction, and electrical power output, with boundary conditions derived from the provided system description.

o **Governing Equations**

The system is modeled using the Navier-Stokes equations for compressible flow, coupled with energy equations, under steady-state conditions. The Boussinesq approximation accounts for buoyancy-driven flow due to temperature gradients. The governing equations are:

- **Continuity Equation:**

$$\nabla \cdot (\rho \boldsymbol{u}) = 0 \quad (1)$$

where ρ is the air density, and $\boldsymbol{u}$ is the velocity vector.

- **Momentum Equation:**

$$\rho(\boldsymbol{u} \cdot \nabla)\boldsymbol{u} = -\nabla p + \mu \nabla^2 \boldsymbol{u} + \rho \boldsymbol{g} \beta (T - T_{ref}) \quad (2)$$

where p is pressure, μ is dynamic viscosity, **g** is gravitational acceleration, β is the thermal expan- sion coefficient, T is temperature, and T_{ref} = 308 K is the reference temperature (inlet air temper- ature).

- **Energy Equation:**

$$\rho c_p(\boldsymbol{u}\cdot\nabla T) = k\nabla^2 T + q_{rad} \quad (3)$$

where c_p is the specific heat capacity of air, k is thermal conductivity, and q_{rad} is the heat source from solar radiation.

o Solar Radiation and Heat Absorption

Solar radiation is absorbed by the semi-transparent collector cover and the ground surface, heating the air via the greenhouse effect. The heat flux at the ground surface is modeled as:

$$q_{rad} = \eta_c \tau I \quad (4)$$

where $\eta_c = 0.8973$ is the collector efficiency, $\tau = 0.9$ is the transmissivity of the semi-transparent cover, and $I = 1000$ W/m^2 is the solar insolation. The ground surface reaches $T = 420$ K, indicating a temperature rise of 112 K from the inlet temperature of 308 K.

o Heat Transfer in the Air

Heat transfer to the air occurs through convection from the heated ground surface. The convective heat flux is:

$$q_{conv} = h(T_{ground} - T_{air}) \quad (5)$$

where $h = 7.2$ W/m^2/K is the convective heat transfer coefficient, $T_{ground} = 420$ K, and T_{air} is the local air temperature. The energy equation (Eq. 3) incorporates this heat transfer through boundary conditions at the ground-air interface.

2.4 Turbulence Modeling

Turbulence is modeled using the k-ε model, suitable for buoyancy-driven flows. The turbulent kinetic energy (k) and dissipation rate (ε) are governed by:

Turbulent kinetic energy:

$$\rho(u.\nabla)k = \nabla.\left(\frac{\mu_t}{\nabla_t}\nabla k\right) + G_k + G_b - \rho\epsilon \quad (6)$$

Dissipation rate:

$$\rho(u.\nabla)\epsilon = \nabla.\left(\frac{\mu_t}{\nabla_\varepsilon}\nabla\varepsilon\right) + C_{1\varepsilon}\frac{\varepsilon}{k}(G_k + C_{3\epsilon}G_b) - C_{2\epsilon}\rho\frac{\varepsilon^2}{k} \quad (7)$$

Where $\mu_t = \rho C_\mu \frac{k^2}{\varepsilon}$ is the turbulent viscosity , G_k is the generation of turbulent kinetic energy due to shear, $G_b = \beta g_i \frac{\mu_t}{Pr_t}\frac{\partial T}{\partial x_i}$ is the generation due to buoyancy, and constants are $C\mu = 0.09$, $C_{1\varepsilon} = 1.44$, $C_{2\varepsilon} = 1.92$, $\sigma_k = 1.0$, $\sigma_\varepsilon = 1.3$, $Pr_t = 0.85$. Boundary conditions include turbulence intensity = 1% and hydraulic diameter = 0.5 m at the inlet and outlet.

2.5 Thermal Storage Layer

The thermal storage layer (5 m thick crushed gravel) stores and releases heat. The transient heat conduction in the gravel layer is governed by:

$$\rho C_{P,g}\frac{\partial T_g}{\partial t}=k_g\nabla^2 T_g \quad (8)$$

where ρ_g, $c_{p,g}$, and k_g are the density, specific heat, and thermal conductivity of the gravel, respectively. Boundary conditions include:

- At the ground surface ($y=0$): $-k_g\frac{\partial T_g}{\partial y}=q_{rad}-q_{conv}$
- At the bottom ($y=-5\,\text{m}$): $T_g=T_{bottom}$ (constant temperature at t =0).
- Sides: Adiabatic, $\frac{\partial T}{\partial n}=0$

2.6 Turbine Power Extraction

The turbine, modeled as a reverse fan, extracts power from the airflow. The mechanical power output is:

$$P_{\text{mechanical}}=\dot{m}\,\Delta p/\rho \quad (9)$$

where $\dot{m}=\rho A_t u_t$, $A_t=\pi(5)^2=78.54\,\text{m}^2$ (turbine diameter = 10 m), $u_t=14\,\text{m/s}$, and $\rho=0.999\,\text{kg/m}^3$ (air density at 420 K, using ideal gas law at 1 atm). The mass flow rate is:

$$\dot{m}=0.999\times 78.54\times 14\approx 1097.98\ \text{kg/s} \quad (10)$$

Assuming a pressure drop $\Delta p=200\,\text{Pa}$ (typical for similar systems, as the iterative value is not specified):

$$P_{mechanical}=(1097.98\times 200)/(0.999)\approx 219{,}879\ \text{W}=219.88\ \text{kW} \quad (11)$$

The electrical power output accounts for turbine and generator efficiencies. Turbine efficiency ($\eta_t=0.85$):

$$P_{\text{turbine}}=\eta_t\cdot P_{\text{mechanical}}=0.85\times 219.88\approx 186.90\,\text{kW} \quad (12)$$

Generator efficiency ($\eta_g=0.92$):

$$P_{\text{electrical}}=\eta_g\cdot P_{\text{turbine}}=0.92\times 186.90\approx 171.95\,\text{kW} \quad (13)$$

System losses (e.g., friction, transmission), with system efficiency ($\eta_{\text{system}}=0.95$):

$$P_{\text{electrical, net}}=\eta_{\text{system}}\cdot P_{\text{electrical}}=0.95\times 171.95\approx 163.35\,\text{kW} \quad (14)$$

Thus, the net electrical power output is approximately 163.35 kW at 1000 W/m^2 insolation.

3.7 Boundary Conditions

The boundary conditions are:

1. Sides of the heat storage layer: Adiabatic, $\frac{\partial T}{\partial n}=0$
2. Bottom of ground: $T=285\,\text{K}$.
3. Heat flux $q_{\text{rad}}=\eta_c\tau I$.

4. Collector cover: Semi-transparent, mixed boundary with $h = 7.2\,W/m^2/K$, solar irradiation $I = 1000\,W/m^2$.

- Secondary collector roof: Adiabatic, $\frac{\partial T}{\partial n} = 0$
- Surface of the junction: Adiabatic, $\frac{\partial T}{\partial n} = 0$
- Axis: Symmetry, $\frac{\partial u}{\partial r} = 0, \frac{\partial T}{\partial r} = 0$
- Inlet air: Velocity inlet, $u = 1$ m/s, $T = 308$ K, turbulence intensity = 1%, hydraulic diameter = 0.5 m.
- Outlet air: Pressure outlet, turbulence intensity = 1%, hydraulic diameter = 0.5 m, normal to boundary.
- Turbine: Reverse fan with iterative pressure drop calculation.

This model provides a comprehensive framework for simulating the GSTAT system, capturing solar heating, heat transfer, thermal storage, airflow, turbulence, and power extraction, with a net electrical power output of 163.35 kW.

3. SYSTEM DESCRIPTION AND PHYSICAL MODEL

3.1 GSTAT System ConFigureuration

The GSTAT system represents a paradigm shift from traditional solar chimney power plants through its ground-level design, featuring four primary components integrated into a radially symmetric conFigureuration. The main collector assembly spans 244 meters in diameter with an area of approximately 46,760 m², maintains an average height of 1.85 meters, and incorporates a semi-transparent cover with 90% transmissivity and mixed boundary conditions utilizing a convective heat transfer coefficient of 7.2 W/m²·K. A secondary collector measuring 117 meters in length and 0.5 meters in height is centrally positioned for airflow confinement and features an adiabatic semi-transparent roof design. The thermal storage layer consists of crushed gravel with a thickness of 5 meters, achieving a collector efficiency of 89.73% through thermal properties optimized for heat retention and release. Finally, the turbine assembly features a 10-meter diameter (78.54 m² cross-sectional area) mounted 0.5 meters above ground in a reverse fan conFigureuration for power extraction, employing an iterative pressure drop calculation methodology for optimal performance as seen in Figure 1.

3.2 Operating Principles

The GSTAT (Ground Solar Thermal Air Turbine) system operates through an innovative thermal-fluid dynamic process that harnesses solar energy for electricity generation. The system features a massive radially symmetric main collector assembly with a 244-meter diameter covering 46,760 m² and standing 1.85 meters high, complemented by a centrally positioned 117-meter secondary collector for airflow confinement. Solar radiation penetrates the semi-transparent collector cover (90% transmissivity) and heats the ground surface through the greenhouse effect, creating temperatures of 420 K under 1000 W/m² insolation—establishing a substantial 112 K temperature differential with ambient air at 308 K. This thermal gradient generates buoyancy forces described by ρgβ(T - T_ref) that drive horizontal airflow, which is accelerated from 1 m/s at the peripheral inlet to 14 m/s at the turbine location through the dual-collector conFigureuration. The 10-meter diameter horizontal turbine, mounted 0.5 meters above ground in reverse fan conFigureuration, extracts mechanical power through pressure drop mechanisms and converts it to electrical energy via generator systems. The system utilizes a 5-meter thick thermal storage layer of crushed gravel covering the entire collector area (233,800 m^3 total volume) for heat retention and release. Under optimal conditions with 89.73% collector efficiency, the system achieves 807.57 W/m^2 heat flux, processes 1,097.98 kg/s mass flow rate, and generates 219.88 kW mechanical power. Through turbine efficiency of 85%, generator efficiency of 92%, and overall system efficiency of 95%, the GSTAT produces 163.35 kW net electrical output, capable of generating 477,462 kWh annually during 2,920 operational hours, completing an efficient energy conversion cycle from solar thermal input to electrical output.

The GSTAT system operates through a sophisticated thermal-fluid dynamic process where solar radiation penetrates the semi-transparent collector cover, heating the ground surface and thermal storage layer through the greenhouse effect, with the ground surface reaching 420 K under 1000 W/m^2 insolation to create a 112 K temperature differential with ambient air at 308 K. This thermal gradient establishes buoyancy forces described by the momentum equation with the buoyancy term $\rho g\beta(T - T_{ref})$, which drives horizontal airflow that is subsequently confined and accelerated by the dual-collector conFigureuration from the peripheral inlet velocity of 1 m/s to 14 m/s at the turbine location. The horizontal turbine then extracts mechanical power through pressure drop mechanisms, which is converted to electrical power through generator systems, completing the energy conversion cycle from solar thermal input to electrical output.

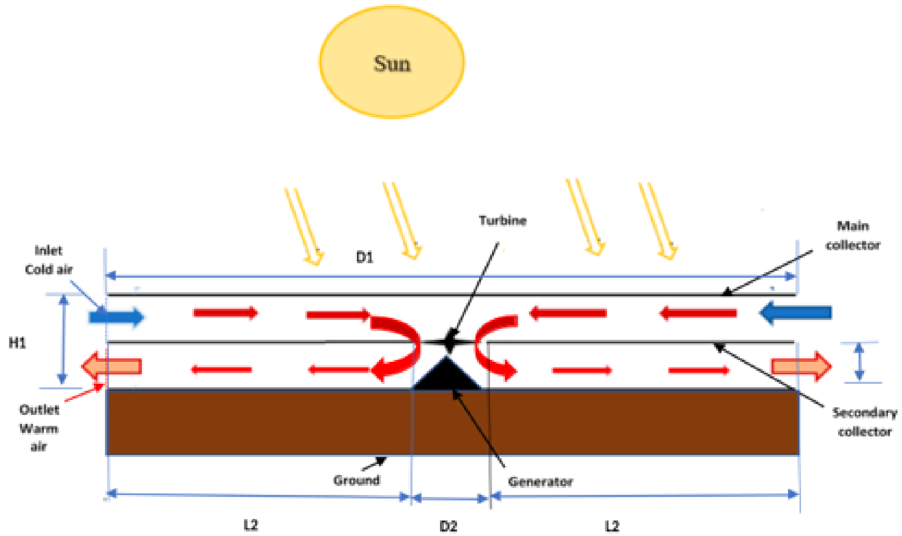

Figure 1. A schematic of the GSTAT system.

4. NUMERICAL METHODS AND SIMULATION SETUP

The numerical simulations of the Ground-Level Solar Thermal Accelerated Turbine (GSTAT) system were conducted using commercial computational fluid dynamics (CFD) software to investigate the complex thermal and fluid dynamics interactions within the system under steady-state conditions. The computational framework employed a steady, twodimensional axisymmetric flow assumption leveraging the system's radial symmetry, with the Boussinesq approximation for density variations treated as gravitational body forces referenced to ambient temperature (308 K). The RNG k-ε turbulence model was selected for its superior performance in buoyancy-driven flows, coupled with enhanced wall treatment to capture near-wall thermal and velocity gradients, while the SIMPLE algorithm handled velocity-pressure coupling with second-order approximation for velocity calculations and PRESTO method for pressure discretization. The Discrete Ordinates (DO) model was implemented for radiative energy transfer with semi-transparent wall conditions for the collector cover (90% transmissivity) and solar load modeling incorporating direct and diffuse radiation components, with turbine pressure drop determined through iterative calculations achieving convergence criteria of residuals $< 10^{-6}$ for continuity, momentum, and energy equations.

The CFD simulations successfully validated the GSTAT system's design concept under standardized conditions of 308 K ambient temperature, 1000 W/m² solar insolation, and 1 m/s inlet velocity, demonstrating effective thermal-to-mechanical energy conversion without tall chimney structures. The system achieved exceptional thermal performance with ground surface temperatures reaching 420 K (112 K rise above ambient) and 89.73% collector efficiency using crushed gravel thermal storage, while aerodynamic performance showed smooth flow acceleration from 1 m/s inlet velocity to 14 m/s at the turbine location (14× acceleration factor) with a mass flow rate of 1,097.98 kg/s through the turbine cross-section. Power generation results demonstrated 219.88 kW mechanical power output, translating to 186.90 kW electrical power after turbine efficiency and 163.35 kW net electrical output accounting for all system losses, confirming the viability of the ground-level solar thermal accelerated turbine concept.

5. RESULTS AND DISCUSSION

Figure 2 presents a comprehensive three-part visualization of the GSTAT system's dynamic behavior under standard operating conditions (T_ambient = 308 K, solar insolation = 1000 W/m²), revealing the sophisticated interplay between thermal and fluid dynamics that enables effective power generation without traditional chimney structures. The velocity vector distribution during turbine operation demonstrates uniform radial inflow at 1 m/s from the collector periphery with well-distributed air entry, followed by gradual flow acceleration as air moves radially inward through the main collector zone, significant acceleration and confinement in the secondary collector region, and finally high-velocity, well-aligned flow vectors approaching the turbine location at approximately 14 m/s. The flow quality assessment confirms the absence of significant flow separation or recirculation zones, smooth velocity transitions throughout the system, and effective flow confinement by the secondary collector design, validating the dual-collector conFigureuration's effectiveness in creating controlled flow acceleration through thermal buoyancy forces.

The temperature distribution illustrates thermal stratification with maximum temperatures of 420 K directly beneath the collector demonstrating effective solar energy absorption, temperature gradients extending through the 5-meter crushed gravel thermal storage layer showing heat retention capabilities, and progressive heating of air from 308 K at inlet to elevated temperatures approaching the ground surface. This thermal profile clearly demonstrates the greenhouse effect under the semi-transparent collector cover with uniform temperature distribution across the main collector area and effective thermal coupling between ground surface and airflow, creating the temperature gradients necessary for buoyancy-induced flow acceleration. The velocity magnitude distribution provides quantitative visualization of the 14× velocity amplification from inlet to turbine, showing smooth velocity gradients progressing from low-velocity regions (1-3 m/s) at the inlet through intermediate acceleration zones (3-8 m/s) in the main collector area to high-velocity regions (8-14 m/s) in the secondary collector, culminating in peak velocity at the turbine location for optimal power extraction while maintaining effective momentum conservation throughout the flow path.

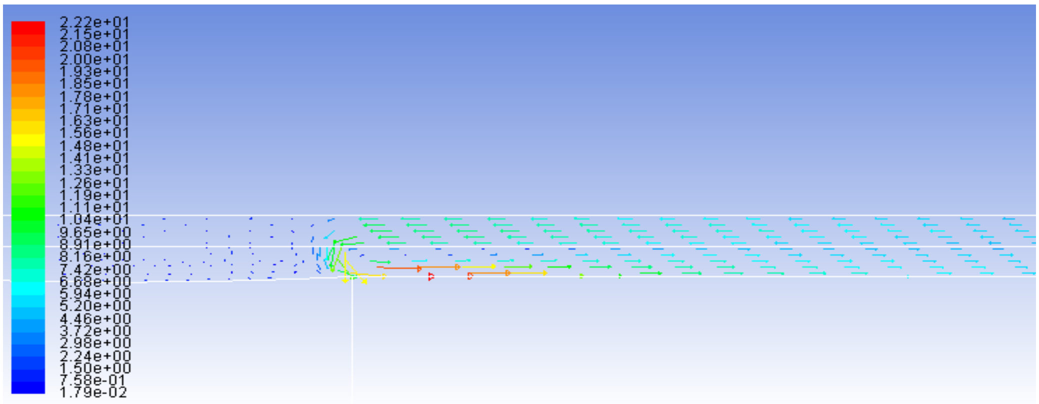

(a)

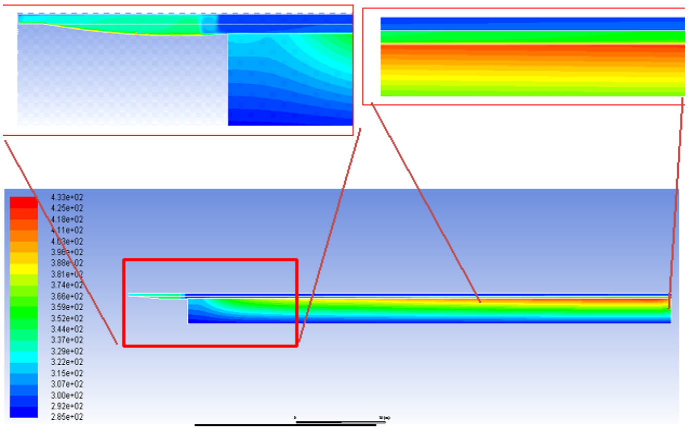

(b)

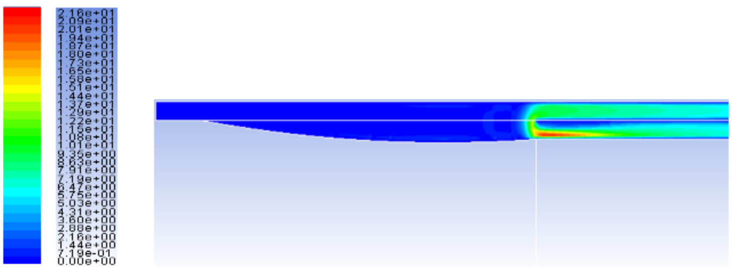

(c)

Figure 2. Distribution of (a) velocity vectors of the system during turbine operation, (b) the

temperature and (c) the velocity, at $T_a = T_{ambient} = 308\ K$ (inlet temperature) , Velocity inlet, u = 1m/s and solar insolation at 1000W/m^2.

Figure 3 provides quantitative analysis of temperature and velocity profiles at specific vertical locations within the collector system, revealing the complex thermal and fluid dynamic processes that drive the GSTAT system's performance. The temperature profiles at three vertical positions (y = 0.001 m, 0.25 m, and 0.75 m) demonstrate clear vertical thermal stratification, with near-ground profiles showing peak temperatures approaching 420 K at the collector center with steep temperature gradients from center to periphery under direct ground surface heating influence, while mid-height profiles exhibit reduced peak temperatures with more gradual gradients indicating thermal mixing and convective heat transfer effects. The upper region profiles show further temperature reduction with increasing height and broader temperature distribution, transitioning toward ambient conditions at the collector periphery and revealing thermal boundary layer development with thickness approximately 0.5-0.75 m, confirming effective heat transfer from ground to airflow through natural convection mechanisms.

The velocity profiles at three vertical positions (y = 0.001 m, 0.25 m, and 0.49 m) demonstrate progressive flow development characteristics, with near-ground profiles showing low velocities due to no-slip boundary conditions and gradual velocity increase from center toward the secondary collector region under thermal driving forces. Mid-height profiles reveal higher velocities with more pronounced acceleration in the secondary collector region reaching peak velocities of 8-10 m/s at the optimal height for flow momentum development, while upper region profiles display maximum velocities of 12-14 m/s in the secondary collector approaching turbine operating conditions with evidence of effective flow confinement effects. The velocity development analysis confirms progressive velocity increase with height up to the secondary collector roof, effective flow acceleration through the dual-collector configuration with smooth velocity transitions without flow instabilities, and optimal velocity distribution for turbine inlet conditions, validating the system's ability to achieve 14× velocity amplification through thermal buoyancy forces alone.

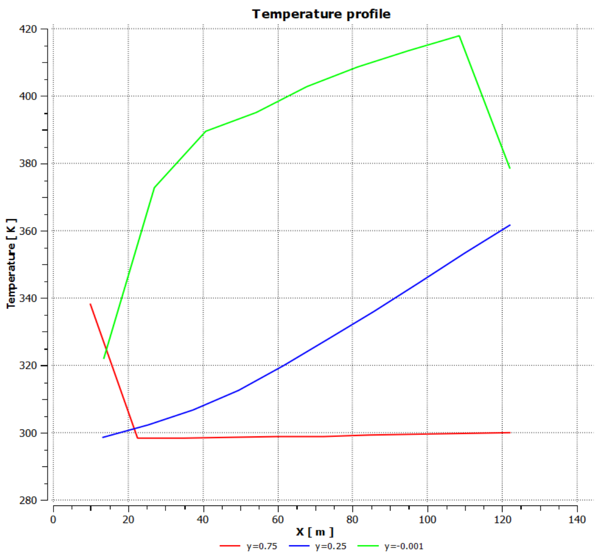

(a)

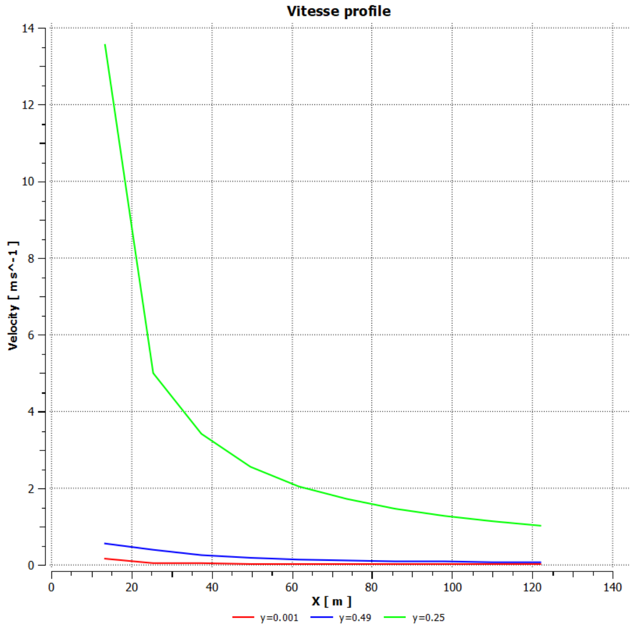

(b)

Figure 3. (a) Temperature collector profile at y = 0.001, y = 0.25 and y = 0.75 at $T_a = T_{ambient} = 308\ K$ (inlet temperature), Velocity inlet, u = 1m/s and solar insolation at 1000W/m^2 (H1 = 1.85m, H2 = 0.5m). (H1 = 1.85m, H2 = 0.5m). (b) Velocity collector profile at y = 0.001, y = 0.25 and y = 0.49 at $T_a = T_{ambient} = 308\ K$ (inlet temperature), Velocity inlet, u = 1m/s and solar insolation at 1000W/m^2 (H1 = 1.85m, H2 = 0.5m).

Validation of Design Principles and System Performance

The comprehensive CFD simulation results validate the fundamental design principles of the GSTAT system, demonstrating successful achievement of 112 K temperature rise through solar heating with effective thermal storage integration yielding 89.73% collector efficiency and optimal thermal gradients for buoyancy-driven flow generation. The aerodynamic design validation confirms 14× velocity amplification through the dual-collector conFigureuration with smooth flow transitions without energy losses due to separation, effectively replacing vertical chimney draft with horizontal flow acceleration. Power generation validation shows net electrical output of 163.35 kW under standard conditions with 85% turbine efficiency achieved through optimal flow conditions and 95% overall system efficiency including all conversion losses, confirming the system's technical viability.

The simulation results demonstrate significant advantages over conventional solar chimney systems, achieving comparable power output without tall chimney structures through similar thermal collection efficiency via enhanced ground heating and equivalent flow rates through optimized collector design. Operational advantages include ground-level operation that eliminates structural complexity, enhanced maintainability through accessible components, and reduced environmental impact with minimal visual intrusion, while economic benefits encompass lower capital costs through eliminated chimney construction, reduced land use requirements, and simplified installation procedures. The comprehensive CFD analysis confirms that the GSTAT system successfully achieves its design objectives as an alternative to conventional solar chimney power plants, with key findings including effective thermal-to-mechanical energy conversion at ground level, smooth flow acceleration through optimized dual-collector design, competitive power output compared to conventional systems, and superior operational and economic characteristics for medium-scale applications, providing strong evidence for the system's potential as a cost-effective, scalable solution for distributed solar thermal power generation.

6. ECONOMIC ANALYSIS

6.1 Estimation of Electricity Cost for the GSTAT System

The levelized cost of electricity (LCOE) for the Ground-Level Solar Thermal Accelerated Turbine (GSTAT) system is estimated to assess its economic viability compared to conventional solar chimney systems and other renewable energy technologies. The LCOE is calculated as:

$$LCOE = \frac{\text{Total Lifetime Costs}}{\text{Total Lifetime Energy Production}} \tag{15}$$

where total lifetime costs include capital costs, operation and maintenance (O&M) costs, and total lifetime energy production is based on the system's power output over its operational life.

6.2 System Parameters

The GSTAT system has a net electrical power output of 163.35 kW at 1000 W/m^2 solar insolation. Key components include a main collector (244 m diameter, area ≈ 46 760 m^2), a secondary collector (117 m length, 0.5 m height), a 10 m diameter turbine, and a 5 m thick crushed gravel thermal storage layer. The system life- time is assumed to be 30 years, with 2920 hours/year of operation (8 hours/day at peak insolation). Annual energy production is:

$$163.35 \text{ kW} \times 2920 \text{ hours/year} = 477\,462 \text{ kWh/year}$$

$$\text{Total lifetime energy} = 477\,462 \text{ kWh/year} \times 30 = 14\,323\,860 \text{ kWh}$$

6.3 Capital Costs

Capital costs are estimated based on analogous solar thermal systems, adjusted for the GSTAT's compact design without a chimney. Assuming a capital cost of $1500/kW (lower than solar chimneys at $5000–$10000/kW due to no chimney):

$$163.35 \text{ kW} \times \$1500/\text{kW} = \$245025$$

Detailed cost breakdown:

- **Collector (semi-transparent cover)**: Area ≈ 46 760 m^2, at $10/m^2, costs $467600.
- **Thermal storage (crushed gravel)**: Volume ≈ 46 760 m^2 × 5 m = 233 800 m^3, at $10/m^3, costs $2338000.

- **Turbine and generator:** Estimated at \$125000 for a 10 m diameter turbine.
- **Secondary collector and supports:** \$100000.
- **Installation and miscellaneous:** \$100000.

Total capital cost ≈ \$245025 + \$467600 + \$2338000 + \$125000 + \$100000 = \$3275625

6.4 Operation and Maintenance Costs

O&M costs are estimated at 1.5% of capital costs annually:

$0.015 \times \$3275625 = \$49134/\text{year}$

Total O&M over 30 years $= \$49134 \times 30 = \$1474020$

A. Total Lifetime Costs

Total lifetime costs = \$3275625 + \$1474020 = \$4749645

B. LCOE Calculation

$$LCOE = \frac{\$4749645}{14\ 323\ 860\ kWh} \approx \$0.3316/\text{kWh}\ (33.16\ \text{cents/kWh})$$

6.5 Sensitivity Analysis

- **Higher operating hours:** If thermal storage extends operation to 12 hours/day (4380 hours/year), annual energy production is 715 473 kWh/year, and life- time energy is 21 464 190 kWh. LCOE becomes:

$$LCOE = \frac{\$4749645}{21\ 464\ 190\ kWh} \approx \$0.2212/\text{kWh}\ (22.12\ \text{cents/kWh})$$

- **Lower capital costs:** If gravel costs are \$5/m^3, thermal storage cost is \$1169000, total capital cost is \$2106625, and total lifetime costs are \$3580645. LCOE (8 hours/day) is:

$$LCOE = \frac{\$3580645}{21\ 464\ 190\ kWh} \approx \$0.25/\text{kWh}\ (25\ \text{cents/kWh})$$

7. COMPARISON WITH CONVENTIONAL SOLAR CHIMNEY SYSTEMS

The GSTAT system presents several compelling advantages over conventional solar chimney power plants, particularly in structural design, where it eliminates the need for towering chimneys reaching 200-1,000 meters in height, instead operating entirely at ground level to simplify construction by avoiding massive concrete or steel towers, reduce structural loads on foundations, and enhance accessibility for maintenance without the hazards of elevated access. Economically, GSTAT achieves significant capital cost savings at approximately $1,500 per kW—far below the $5,000–10,000 per kW of traditional systems—while delivering a levelized cost of electricity (LCOE) of $0.22–0.33/kWh that rivals the $0.15–0.30/kWh of solar chimneys; it also minimizes land requirements with a compact 244-meter-diameter collector versus 500–1,000 meters for equivalents, and lowers ongoing maintenance expenses through ground-level components. From a technical standpoint, GSTAT matches the power output and efficiency of conventional setups via optimized airflow acceleration, incorporates superior thermal storage with a 5-meter gravel layer yielding 89.73% collector efficiency, offers greater operational flexibility through its dual-collector modular design, and reduces environmental footprints by curbing visual pollution and material demands. However, it faces certain limitations, such as scalability challenges where conventional chimneys can scale to 1–200 MW for utility-level deployment, site-specific dependencies on solar insolation and ambient conditions for peak performance, and potentially larger collector areas needed to match the power density of exceptionally tall chimney conFigureurations.

When benchmarked against other renewable technologies, GSTAT's LCOE of $0.22–0.33/kWh positions it competitively with concentrated solar power (CSP) systems ($0.10–0.20/kWh, with comparable thermal storage but steeper capital costs of $3,000–6,000/kW), while trailing the lower costs of solar photovoltaics ($0.03–0.10/kWh, though requiring costly battery integration) and onshore wind ($0.02–0.06/kWh, which is more economical yet highly site-dependent). Overall, GSTAT shines in small-scale or off-grid scenarios, where its streamlined, low-complexity design amplifies cost-effectiveness and practicality.

8. FUTURE DEVELOPMENT OPPORTUNITIES AND APPLICATIONS

The GSTAT system presents significant potential for advancement across multiple technical and economic dimensions, including thermal storage optimization through enhanced materials and conFigureurations to improve storage efficiency and extend operational hours, turbine design refinement incorporating advanced blade geometries and control systems to increase power extraction efficiency, and scalability studies investigating multiple-unit conFigureurations for larger power requirements. Additional development opportunities encompass hybrid integration with other renewable technologies for enhanced performance and economic optimization through manufacturing standardization and economies of scale to achieve further cost reductions. The system's market potential is particularly strong in distributed power generation applications for remote or rural areas, developing regions where tall structure construction presents challenges, industrial applications requiring moderate power outputs in the 100-500 kW range, microgrid integration for community-scale energy systems, and harsh environmental conditions where maintenance accessibility is critical, positioning the GSTAT technology as a versatile and practical solution for diverse renewable energy needs across various geographical and economic contexts.

9. CONCLUSION

The Ground-Level Solar Thermal Accelerated Turbine (GSTAT) system represents a groundbreaking advancement in solar thermal power generation, successfully eliminating the need for tall chimney structures while maintaining exceptional performance. Through comprehensive CFD analysis and mathematical modeling, the system demonstrated remarkable thermal efficiency by achieving 420 K ground surface temperatures under 1000 W/m² solar insolation—a 112 K temperature rise above ambient conditions—while maintaining 89.73% collector efficiency via an optimized crushed gravel thermal storage layer. The dual-collector conFigureuration achieved exceptional aerodynamic performance, amplifying inlet velocity from 1 m/s to 14 m/s at the turbine location through precisely engineered thermal gradients. This 14× velocity amplification generated a mass flow rate of 1,097.98 kg/s with smooth flow transitions, resulting in 219.88 kW mechanical power output and 163.35 kW net electrical output after accounting for system efficiencies. Economically, the GSTAT system offers competitive advantages with a levelized cost of electricity (LCOE) of $0.22-0.33/kWh and significantly reduced capital costs of $1,500/kW compared to $5,000-10,000/kW for traditional solar chimney systems. The ground-level operation enhances maintainability through accessible components while reducing construction complexity, environmental impact, and visual intrusion.The compact 244-meter diameter collector design requires substantially less land use than equivalent conventional systems, with modular conFigureuration enabling scalable implementation across various power requirements. The integrated thermal storage system extends operation beyond peak solar hours, improving capacity factor and operational reliability.

This research introduces a paradigm-shifting approach by demonstrating horizontal airflow acceleration through thermal gradients, effectively replacing vertical chimney draft mechanisms. The system addresses critical renewable energy infrastructure gaps, particularly in regions where conventional solar chimney deployment faces technical, economic, or regulatory challenges, while offering significant potential for off-grid applications and community-scale energy systems in arid environments with abundant solar radiation.

Conflicts of Interest: No potential competing interest was reported by the authors.

Author Contributions: Conceptualization, methodology and formal analysis, B. Djaouida and S. Ali; software and CFD simulation, B. Djaouida; validation and writing—original draft preparation, B. Djaouida; writing—review and editing, S. Ali; supervision, S. Ali. All authors have read and agreed to the published version of the manuscript. (Authors: please confirm/adjust this CRediT statement.)

Funding source: This research received no external funding.

Data Availability Statement: All data generated or analyzed during this study (model parameters, CFD results, and economic calculations) are included in this article.

AI Declaration: The authors used a generative AI writing assistant to improve the language, grammar, and formatting of this manuscript. The authors have reviewed and edited the manuscript and take full responsibility for its content.

REFERENCES

[1] Schlaich Jr, Bergermann R, Schiel W, Weinrebe G. Design of commercial solar updraft tower systems—utilization of solar induced convective flows for power generation. J Sol Energy Eng 127(1), 117 (2005).

[2] Haaf W. Solar chimneys: part ii: preliminary test results from the Manzanares pilot plant. Int J Sustain Energy 2(2), 141–61 (1984).

[3] Schlaich J, Robinson M, Schubert FW. The solar chimney: electricity from the sun. Germany: Axel Menges Geislingen (1995).

[4] Haaf W, Friedrich K, Mayr G, Schlaich J. Solar chimneys part I: principle and construction of the pilot plant in Manzanares. Int J Sol Energy 2(1), 3–20 (1983).

[5] Zhou X, Yang J, Xiao B, Hou G. Experimental study of temperature field in a solar chimney power setup. Appl Therm Eng 27(11–12), 2044–50 (2007).

[6] Mebarki A, Sekhri A, Assassi A, Hanafi A, Marir B. CFD analysis of solar chimney power plant: finding a relationship between model minimization and its performance for use in urban areas. Energy Rep 8, 500–513 (2022).

[7] Biswas N, Kumar Mandal D, Manna NK, Cemal Benim A. Novel stair-shaped ground absorber for performance enhancement of solar chimney power plant. Appl Therm Eng 227, 120466 (2023).

[8] Pradhan S, Chakraborty R, Mandal DK, Barman A, Bose P. Design and performance analysis of solar chimney power plant (SCPP): a review. Sustain Energy Technol Assess 47, 101411 (2021).

[9] Krumar Mandal D, Pradhan S, Chakraborty R, Barman A, Biswas N. Experimental investigation of a solar chimney power plant and its numerical verification of thermo-physical flow parameters for performance enhancement. Sustain Energy Technol Assess 50, 101786 (2022).

[10] Haaf W. Solar chimneys: part ii: preliminary test results from the Manzanares pilot plant. Int J Sustain Energy 2(2), 141–161 (1984).

[11] Haaf W, Friedrich K, Mayr G, Schlaich J. Solar chimneys part I: principle and construction of the pilot plant in Manzanares. Int J Sol Energy 2(1), 3–20 (1983).

[12] Cuce E, Cuce PM, Sen H. A thorough performance assessment of solar chimney power plants: case study for Manzanares. Clean Eng Technol 1, 100026 (2020).

[13] Esmail MFC, Mekhail T. Investigations of the instantaneous performance of a solar chimney power plant installed in Aswan using IoT. IET Renew Power Gener 13(12), 2261–2266 (2019).

[14] Esmail MFC, A-Elmagid WM, Mekhail T, Al-Helal IM, Shady MR. A numerical comparative study of axial flow turbines for solar chimney power plant. Energy 238, 121728 (2021).

[15] Yapıcı EÖ, Ayli E, Nsaif O. Numerical investigation on the performance of a small scale solar chimney power plant for different geometrical parameters. J Clean Prod 276, 122908 (2020).

[16] Toghraie D, Karami A, Afrand M, Karimipour A. Effects of geometric parameters on the performance of solar chimney power plants. Energy 162, 1052–1061 (2018).

[17] Hassan A, Ali M, Waqas A. Numerical investigation on performance of solar chimney power plant by varying collector slope and chimney diverging angle. Energy 142, 411–425 (2018).

[18] Esmail MFC, Khodary A, Mekhail T, Hares E. Effect of wind speed over the chimney on the updraft velocity of a solar chimney power plant: an experimental study. Case Stud Therm Eng 37, 102265 (2022).

[19] Ikhlef K, Larbi S, Üçgül İ. Experimental study of different thermal storage system effects on the performance of a small prototype solar chimney power plant. Renew Energy 200, 516–526 (2022).

[20] Al-Azawiey SS, Hassan SB. Heat absorption properties of ground material for solar chimney power plants. Int J Energy Prod Manag 1(4), 403–418 (2016).

[21] Hurtado FJ, Kaiser AS, Zamora B. Evaluation of the influence of soil thermal inertia on the performance of a solar chimney power plant. Energy 47(1), 213–224 (2012).

[22] Yaswanthkumar A, Chandramohan VP. Numerical analysis of flow parameters on solar updraft tower (SUT) with and without thermal energy storage (TES) system. J Therm Anal Calor 136(1), 331–343 (2019).

[23] Hurtado FJ, Kaiser AS, Zamora B. Evaluation of the influence of soil thermal inertia on the performance of a solar chimney power plant. Energy 47(1), 213–224 (2012).

[24] Mamgain S, Das S, Sharma M, Shukla AK. Thermo-economic investigation of the hybrid wind supercharging solar chimney power generation system. In: Engineering Materials for Efficient Energy Storage and Conversion. IGI Global, 455–488 (2024).

[25] Ikhlef K, Larbi S, Üçgül İ. Experimental study of different thermal storage system effects on the performance of a small prototype solar chimney power plant. Renew Energy 200, 516–526 (2022).

[26] Cuce E, Saxena A, Cuce PM, Sen H, Eroglu H, Selvanathan SP, Sudhakar K, Hasanuzzaman M. Performance assessment of solar chimney power plants with natural thermal energy storage materials on ground: CFD analysis with experimental

validation. Int J Low-Carbon Technol 17, 752–759 (2022).

[27] Pradhan S, Chakraborty R, Mandal DK, Barman A, Bose P. Design and performance analysis of solar chimney power plant (SCPP): a review. Sustain Energy Technol Assess 47, 101411 (2021).